

# Discovery of a tight correlation among the prompt emission properties of long Gamma Ray Bursts

C. Firmani<sup>1,2\*</sup>, G. Ghisellini<sup>1</sup>, V. Avila–Reese<sup>2</sup> and G. Ghirlanda<sup>1</sup>

<sup>1</sup>*Osservatorio Astronomico di Brera, via E. Bianchi 46, I-23807 Merate, Italy*

<sup>2</sup>*Instituto de Astronomía, Universidad Nacional Autónoma de México, A.P. 70-264, 04510, México, D.F.*

12 July 2018

## ABSTRACT

We report the discovery of a correlation among three prompt emission properties of Gamma Ray Bursts. These are the isotropic peak luminosity  $L_{\text{iso}}$ , the peak energy (in  $\nu L_\nu$ ) of the time-integrated prompt emission spectrum  $E_{\text{pk}}$ , and the “high signal” timescale  $T_{0.45}$ , previously used to characterize the variability behavior of bursts. In the rest frame of the source the found correlation reads  $L_{\text{iso}} \propto E_{\text{pk}}^{1.62} T_{0.45}^{-0.49}$ . We find other strong correlations, but at the cost of increasing the number of variables, involving the variability and the isotropic energy of the prompt emission. With respect to the other tight correlations found in Gamma Ray Bursts (i.e. between the collimation corrected energy  $E_\gamma$  and  $E_{\text{pk}}$ , the so-called Ghirlanda correlation, and the phenomenological correlation among the isotropic emitted energy  $E_{\text{iso}}$ ,  $E_{\text{pk}}$  and the jet break time  $t_{\text{break}}$ ), the newly found correlation does not require any information from the afterglow phase of the bursts, nor any model-dependent assumption. In the popular scenario in which we are receiving beamed radiation originating in a fireball pointing at us, the found correlation preserves its form in the comoving frame. This helps to explain the small scatter of the correlation, and underlines the role of the local brightness (i.e. the brightness of the visible fraction of the fireball surface). This correlation has been found with a relatively small number of objects, and it is hard to establish if any selection bias affects it. Its connection with the prompt local brightness is promising, but a solid physical understanding is still to be found. Despite all that, we find that some properties of the correlation, which we discuss, support its true existence, and this has important implications for the Gamma Ray Burst physics. Furthermore, it is possible to use such correlation as an accurate redshift estimator, and, more importantly, its tightness will allow us to use it as a tool to constrain the cosmological parameters.

**Key words:** cosmological parameters — cosmology: observations — distance scale — gamma rays: bursts — gamma rays: observations

## 1 INTRODUCTION

A major breakthrough in the understanding of Gamma Ray Burst (GRB) has been the discovery of X-ray, optical and radio counterparts in some long-duration bursts (Costa et al. 1997; van Paradijs et al. 1997; Frail et al. 1997). This allowed to measure their redshifts and realize that they are at cosmological distances. Since then, two potential and appealing possibilities were cherished: the use of GRBs (i) as dust-free tracers of the massive star formation history in the universe (e.g., Totani 1997; Paczynski 1998; Wijers et al. 1998; Lamb & Reichart 2000; Blain & Natarajan 2000; Bromm & Loeb 2002; Lloyd-Ronning, Fryer & Ramirez-Ruiz 2002; Firmani et al.

2004; Yonetoku et al. 2004), and (ii) as cosmological standard candles able to provide a record of the cosmic expansion history up to high redshifts (e.g., Schaefer 2003; Ghirlanda et al. 2004b; Dai, Liang & Xu 2004; Firmani et al. 2005; Liang & Zhang 2005; Xu, Dai & Liang 2005). Both items face the problem of small number of events with measured  $z$ , since to determine it, deep optical/IR or X-ray spectra are needed. Regarding the latter item (ii), the large dispersion of the GRB energetics makes GRBs all but standard candles (Frail et al. 2001; Bloom, Frail & Kulkarni 2003). However, major advances in overcoming both difficulties can be done on the base of tight relations that connect GRB intrinsic energetics and/or luminosities with observed quantities. These relations serve as redshift indicators or, when  $z$  is known independently, to make GRBs standard candles for cosmographic purposes.

\* E-mail: firmani@merate.mi.astro.it

The first proposed GRB luminosity (redshift) indicators were based on the discovery of two empirical relations between the burst isotropic-equivalent luminosity ( $L_{\text{iso}}$ ) and the variability ( $V$ ), which is a measure of the “spikiness” of the  $\gamma$ -ray light curve (Fenimore & Ramirez-Ruiz 2000; Reichart et al. 2001), and between  $L_{\text{iso}}$  and the spectral lag ( $\tau_{\text{ag}}$ ) (Norris, Marani, & Bonnell 2000). Later, Atteia (2003) constructed another redshift indicator based on  $\gamma$ -ray data alone linking the spectral parameters and the duration ( $T_{90}$ ) of the prompt emission, and he showed that it provides pseudo-redshifts accurate within a factor of two. In a study of the energetics of GRBs Lloyd-Ronning & Ramirez-Ruiz (2002a) found the evidence that GRBs with highly variable light curves have greater  $\nu F_\nu$  spectral peak energies. The existence of such a correlation and of the variability–luminosity correlation also implied that the rest frame GRB peak energy  $E_{\text{peak}}$  is correlated with the intrinsic luminosity of the burst. Amati et al. (2002), by analyzing the spectra of *BeppoSAX* GRBs, found that the isotropic-equivalent energy radiated during the prompt phase ( $E_{\text{iso}}$ ) is correlated with the rest-frame peak energy of the  $\gamma$ -ray spectrum [ $E_{\text{pk}} = E_{\text{pk}}^{\text{obs}}(1+z)$ ,  $E_{\text{pk}}^{\text{obs}}$  is in the observer frame]. However, the large scatter of this correlation makes it difficult to use it as a reliable redshift indicator. Yonetoku et al. (2004, see also Ghirlanda et al. 2005) found that there is also some correlation between  $L_{\text{iso}}$  and  $E_{\text{pk}}$ .

Using the above mentioned empirical correlations, hundreds of GRB pseudo-redshifts were estimated from prompt  $\gamma$ -ray observables *and* within a given cosmology. However, due to the lack of enough low- $z$  (calibrator) GRBs, these correlations are themselves cosmology dependent (but see Ghirlanda et al. 2005a). This introduces a circularity problem if the goal is to use these relations as distance-indicators and transform GRBs with measured  $z$  into cosmological rulers: the parameters of the relations depend on the cosmological parameters that we pretend to constrain. To avoid this circular logic, Schaefer (2003) proposed to determine both the GRB and cosmological parameters by fitting simultaneously the model relations to the data, and the cosmological model to the constructed Hubble diagram (luminosity distance  $d_L$  vs  $z$ ). However, as he showed, an accurate determination of the cosmological parameters was not possible due to the large dispersion around the  $L_{\text{iso}} - V$  and  $L_{\text{iso}} - \tau_{\text{ag}}$  relations.

The hope to use GRBs as cosmological rulers renewed after the finding by Ghirlanda, Ghisellini & Lazzati (2004a, hereafter GGL2004) that the Amati correlation becomes much tighter if one corrects  $E_{\text{iso}}$  for the collimation factor of the jet opening angle. The presence of an achromatic break in the GRB afterglow light curves is a strong evidence that the GRB emission is collimated into a cone of semiaperture angle  $\theta_j$  (e.g., Rhoads 1997; Sari, Piran & Halpern 1999), where  $\theta_j$  is the rest frame time of the achromatic break in the lightcurve of the afterglow. Thus, the collimated-corrected  $\gamma$ -ray energetic is  $E_\gamma = (1 - \cos \theta_j)E_{\text{iso}}$ . The  $E_\gamma$ – $E_{\text{pk}}$  correlation, determined with less than 20 GRBs, has been used to put constraints on some cosmological parameters avoiding (Ghirlanda et al. 2004b; Firmani et al. 2005) and not avoiding (Dai, Liang & Xu 2004) the circularity problem.

More recently, Liang & Zhang (2005, hereafter LZ2005) (see also Xu 2005) investigated the correlation among  $E_{\text{iso}}$ ,  $E_{\text{pk}}$ , and  $t_{\text{break}}$  without imposing any theoretical model and

assumptions. They found a purely empirical tight correlation among these quantities which apparently suffers less uncertainties than the Ghirlanda relation, though both correlations are mutually consistent (Nava et al. 2006). These authors used the  $E_{\text{iso}}$ – $E_{\text{pk}}$ – $t_{\text{break}}$  correlation as a luminosity distance indicator and applied their own methods to avoid the circularity problem to constrain some dynamical and kinematical cosmological parameters.

As discussed in Ghisellini et al. (2005) and LZ2005, the future of GRB cosmology is promising (but see Friedman & Bloom 2005), the identification of more and more GRBs with accurately measured  $z$ ,  $E_{\text{pk}}^{\text{obs}}$  and  $t_{\text{break}}^{\text{obs}}$  being crucial. Unfortunately, the determination of  $t_{\text{break}}$  requires expensive follow-up campaigns involving large telescopes. Up to now,  $t_{\text{break}}$  has been measured for about one third ( $\sim 20$ ) of the GRBs with measured  $z$  ( $\sim 60$ ). This motivates the need of developing an astronomical program entirely devoted to measure  $z$ ,  $E_{\text{pk}}$  and  $t_{\text{break}}$  (Lamb et al. 2005). On the other hand, the discovery of tight correlations among the GRB energetics and the prompt  $\gamma$ -ray observables alone (by-passing the need of measuring  $t_{\text{break}}$ ) is of primary interest. This is the main aim of this paper.

In §2, we present the GRB sample used in this work as well as the sample selection criteria. Using this sample, in §3 we revisit the correlation found by LZ2005 among  $E_{\text{iso}}$ ,  $E_{\text{pk}}$  and  $t_{\text{break}}$ . We will later compare this correlation with the one we find using observables which can be extracted by the prompt emission only. In §4 we present our method to characterize the variability of the prompt emission. The search for a multi variable correlation among energetics and the prompt  $\gamma$ -ray observables is presented and analyzed in §5, where we derive the main result of our work, namely a very tight correlation between the peak luminosity of the prompt emission  $L_{\text{iso}}$ , the peak spectral energy  $E_{\text{pk}}$  and the “high signal” timescale  $T_{0.45}$ . In §6 we discuss how this newly found correlation can be used as a rather accurate redshift indicator. The theoretical implications of our findings are discussed in §7. Finally, in §8 we draw our conclusions.

## 2 THE SAMPLE

The study of the correlations among prompt emission observables requires a careful selection of the GRB sample in order to work with a reliable and homogeneous set of information. The basic selection criteria we adopt are the knowledge of:

- (i) the redshift  $z$ ;
- (ii) the peak flux  $P$  and the fluence  $F$ , better if defined both in the same energy range;
- (iii) the  $\nu F_\nu$  peak energy,  $E_{\text{pk}}^{\text{obs}}$ , and a fitting to the spectrum able to provide a reasonable determination of the bolometric correction. Note that  $E_{\text{pk}}^{\text{obs}}$  is derived in all cases using the time integrated spectrum.
- (iv)  $T_{0.45}^{\text{obs}}$  and  $V$ . When possible, these parameters have been calculated with our own code using the published light curves (see below).

The time  $T_{0.45}^{\text{obs}}$  is the prompt “high-signal” timescale, introduced by Reichart et al. (2001, hereafter R2001), defined in the rest energy range 50–300 keV (see §4.1). For comparative purposes, the knowledge of the observed  $t_{\text{break}}^{\text{obs}}$  is also

GRB	Instrument	$z$	Ref.	$T_{90}^{\text{obs}}$	Ref.	$T_{0.45}^{\text{obs}}$	Ref.	$T_{\text{break}}^{\text{obs}}$	Ref.
970228	SAX/WFC	0.695	1	80	27	$2 \pm 1$	33	...	
970828	RXTE/ASM	0.957	2	146.6	27	$14 \pm 2$	33	$2.2 \pm 0.4$	35
971214	SAX/WFC	3.42	3	35	27	$7.3 \pm 0.2$	0	...	
980703	RXTE/ASM	0.966	4	102.4	27	$17.2 \pm 0.3$	0	$3.4 \pm 0.5$	35
990123	SAX/WFC	1.6	5	100	27	$17.2 \pm 0.1$	0	$2.0 \pm 0.5$	36
990506	BAT/PCA	1.307	6	220	27	$14.05 \pm 0.06$	0	...	
990510	SAX/WFC	1.619	7	75	27	$5.00 \pm 0.05$	0	$1.6 \pm 0.2$	37
990705	SAX/WFC	0.843	8	42	27	$5 \pm 2$	33	$1.0 \pm 0.2$	35
990712	SAX/WFC	0.43	7	20	27	...	33	$1.6 \pm 0.2$	38
991216	BAT/PCA	1.02	9	24.9	27	$3.78 \pm 0.02$	0	$1.2 \pm 0.4$	35
000131	Uly/KO/NE	4.5	10	110.1	27	$4 \pm 1$	33	...	
000911	Uly/KO/NE	1.058	11	500	27	$5.2 \pm 0.5$	34	...	
011211	SAX/WFC	2.14	12	...		...	0	$1.5 \pm 0.2$	39
020124	HETE	3.2	13	50	28	$14.0 \pm 1.5$	0	$3.0 \pm 0.4$	40
020813	HETE	1.25	14	90	27	$17 \pm 1$	0	$0.43 \pm 0.06$	41
021211	HETE	1.01	15	13	28	$0.81 \pm 0.05$	0	...	
030226	HETE	1.98	16	138	28	$26 \pm 2$	0	$0.84 \pm 0.10$	41
030328	HETE	1.52	17	316	28	$26.2 \pm 0.7$	0	$0.8 \pm 0.1$	42
030329	HETE	0.1685	18	33	28	$5.0 \pm 0.1$	0	$0.5 \pm 0.1$	43
030429	HETE	2.658	19	77	28	...		$1.8 \pm 1.0$	44
040924	HETE	0.859	20	5	21	$0.45 \pm 0.02$	0	...	
041006	HETE	0.716	21	25	21	$4.47 \pm 0.01$	0	$0.16 \pm 0.04$	45
050525	SWIFT	0.606	22	8.8	29	$2.09 \pm 0.01$	0	$0.15 \pm 0.01$	30
980425	BAT/SAX	0.0085	23	37.4	30	$7.5 \pm 0.2$	0	...	
990712	SAX	0.433	24	20.0	31	$4 \pm 1$	0	$1.6 \pm 0.2$	46
010921	HETE	0.45	25	24.6	21	$7.3 \pm 0.4$	0	...	
031203	INTEGRAL	0.106	26	30	32	$5 \pm 1$	0	...	

**Table 1.**  $T_{90}^{\text{obs}}$ ,  $T_{0.45}^{\text{obs}}$ ,  $T_{\text{break}}^{\text{obs}}$  are expressed in seconds. References: (0) This paper; (1) Djorgovski et al. 1997; (2) Djorgovski et al. 2001; (3) Kulkarni et al. 1998; (4) Djorgovski et al. 1998; (5) Hjorth et al. 1999; (6) Bloom et al. 2001; (7) Vreeswijk et al. 2001; (8) Amati et al. 2000; (9) Vreeswijk et al. 1999; (10) Andersen et al. 2000; (11) Price et al. 2002; (12) Amati et al. 2004; (13) Hjorth et al. 2003; (14) Barth et al. 2003; (15) Vreeswijk et al. 2003; (16) Greiner et al. 2003; (17) Rol et al. 2003; (18) Greiner et al. 2003a; (19) Weidinger et al. 2003; (20) Wiersema et al. 2004; (21) <http://space.mit.edu/HETE/Bursts>; (22) Foley et al. 2005; (23) Tinney et al. 1998; (24) Galama et al. 1999; (25) Djorgovski et al. 2001a; (26) Bersier et al. 2003; (27) Ghirlanda et al. 2004a; (28) Sakamoto et al. 2005; (29) Blustin et al. 2005; (30) Jimenez et al. 2001; (31) Amati et al. 2002; (32) Mereghetti & Gotz 2003; (33) Reichart et al. 2001; (34) Guidorzi et al. 2005; (35) Bloom et al. 2003; (36) Kulkarni et al. 1999; (37) Israel et al. 1999; (38) Bjornsson et al. 2001; (39) Jakobsson et al. 2003; (40) Berger et al. 2002; (41) Klose et al. 2004; (42) Andersen et al. 2003; (43) Berger et al. 2003; (44) Jakobsson et al. 2004; (45) Stanek et al. 2005; (46) Bjornsson et al. 2001.

desirable, although we did not require it as a selection criterion. For the few cases when the observed  $P$  is not available, we have estimated it from the light curve profile by using the published spectrum and fluence.

Our sample includes mainly the GRBs reported in GGL2004 (15 GRBs); in some cases the data of these bursts have been updated with more recent published analysis. To the GGL2004 sample, we have added 7 GRBs. In Table 1 we present the resulting sample of the 22 GRBs used in this paper, specifying the mission/instrument from which the data were acquired and the spectroscopically measured redshift  $z$ . For each burst we report the duration  $T_{90}$ , the  $T_{0.45}^{\text{obs}}$  timescale and the jet break time  $T_{\text{break}}^{\text{obs}}$  in the observer frame. In most cases  $T_{0.45}^{\text{obs}}$  was computed from the GRB light curve as discussed below (§4.1). The data from R2001 were adapted to the 50-300 keV band by interpolation. We have compared our results with the ones of R2001 for the common GRBs finding a good agreement. This comparison has been helpful for us to estimate the uncertainty of the data derived from R2001.

In Table 2, we list the bolometric corrected fluence ( $F$ ) and peak flux ( $P$ ) and the corresponding energy range where

they were computed. In Table 2 we also report the spectral parameters  $\alpha$  and  $\beta$  for those bursts whose spectrum was fitted by the Band et al. (1993) spectral model and only the  $\alpha$  spectral parameter when the spectrum was fitted with a cutoff-powerlaw model. The fluence and the peak flux are given respectively either in units of  $\text{erg cm}^{-2}$  and  $\text{erg cm}^{-2} \text{s}^{-1}$ , in round brackets, or in units of  $\text{photon cm}^{-2}$  and  $\text{photons cm}^{-2} \text{s}^{-1}$ , in square brackets. This choice of homogeneity, as well as the one of the same energy range for the fluence and the peak flux, have been made with the aim to reduce the effects of the spectral uncertainty on the  $L_{\text{iso}}/E_{\text{iso}}$  ratio.

In Table 3 we report the rest frame  $E_{\text{pk}}$ ,  $E_{\text{iso}}$ ,  $L_{\text{iso}}/E_{\text{iso}}$  ratio and  $V$ . The sample has been divided into two classes. Class 1 (16 events) comprises those GRBs with a good determination of the bolometric correction. Class 2 (5 events) comprises those events with uncertain bolometric corrections. In fact, the uncertain high-energy spectrum of Class 2 bursts does not allow to constrain the high-energy Band spectral index ( $\beta$ ). In these cases spectral fits were performed either freezing  $\beta$  to a fiducial value ( $\beta = -2.3$ ) or the fit was performed using a cutoff power law model. For

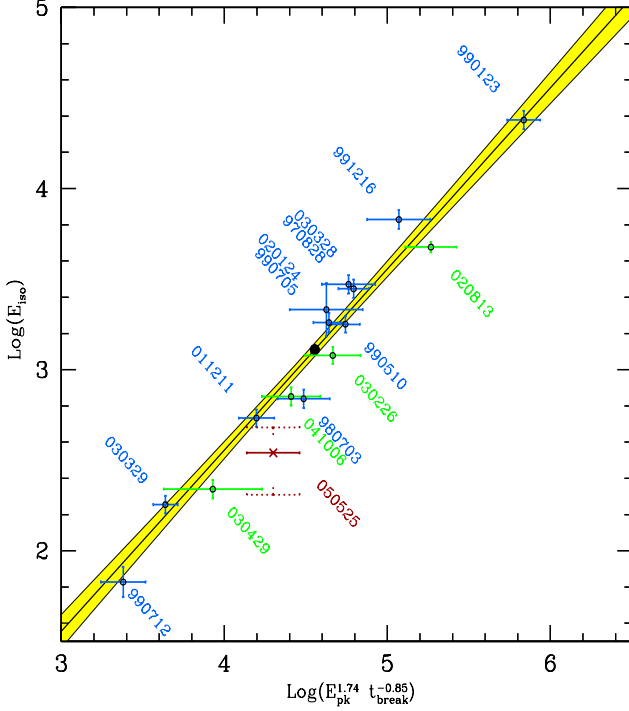


**Figure 1.** Isotropic emitted energy  $E_{\text{iso}}$  as a function of  $E_{\text{peak}}^{1.74} t_{\text{break}}^{-0.85}$  (Eq. 1.). The open circles represent the 15 bursts (i.e. all those with measured  $t_{\text{break}}$  in Tab. 1 except 050525) used for the fit (solid line). The solid filled region represents the  $1\sigma$  uncertainty on the best fit (see Eq. 1). The fit is performed in the centroid defined by the data points (solid circle) where the errors on the best fit parameters are uncorrelated. The color codes are: blue for class 1 bursts, green for class 2 and brown for class 3. For GRB 050525 we also report the values obtained assuming  $\beta = -2.1$  and  $\beta = -5$  (dotted lines).

GRB 050525 we assign a special class, 3, because the determination of  $\beta$  in this case is highly uncertain.

Regarding the uncertainties, for those quantities taken from the observations ( $z$ ,  $F$ ,  $P$ , and  $E_{\text{pk}}^{\text{obs}}$ ), we use the errors reported in the literature. For the derived quantities  $E_{\text{iso}}$ ,  $L_{\text{iso}}$ , and  $\Phi$  (see below), we calculate their uncertainties by propagating the errors under the assumption that they are uncorrelated.

The conventional  $\Lambda$ CDM cosmology with  $\Omega_{\text{M}} = 0.3$ ,  $\Omega_{\Lambda} = 0.7$  and  $h = 0.7$  is assumed here for the calculation of luminosity distances.

### 3 THE $E_{\text{iso}}-E_{\text{pk}}-t_{\text{break}}$ CORRELATION

As stated in the Introduction, our aim is to find a statistically significant (multi)variable correlation among GRB prompt emission observables. Previous to this, we present here for our sample the  $E_{\text{iso}}$ ,  $E_{\text{pk}}$  and  $t_{\text{break}}$  correlation (LZ2005), and discuss some of its implications. We will also attempt later to compare and connect our results to this correlation. Using the same fitting procedure as in Nava et al. (2006) for those 15 events for which  $t_{\text{break}}$  is known, we

obtain the following best fit, in the GRB rest frame:

$$E_{\text{iso}} = 10^{53.11 \pm 0.04} \left( \frac{E_{\text{pk}}}{10^{2.48} \text{keV}} \right)^{1.74 \pm 0.10} \left( \frac{t_{\text{break}}}{10^{-0.29} \text{d}} \right)^{-0.85 \pm 0.15} \text{erg}, \quad (1)$$

with  $\chi_r^2 = 0.67$  (for 12 dof). Notice that, differently from LZ2005, we do take into account for the fit the uncertainties in the data. The data and Eq. (1) are shown in a two dimensional plot in Fig. 1. In our sample, which has been constructed to find correlations among prompt variables alone, GRB 020405 and GRB 021004 are not included because for them the high-energy spectral parameter  $\beta$  is larger than  $-2$  (GRB 020405) or unknown (GRB 021004), (but see Nava et al. 2006). We did not take into account GRB 050525 for the fit of Eq. (1) due the large uncertainty in the  $\beta$  parameter, but we plot it in Fig. 1: the dotted lines correspond to values of  $\beta$  between  $-2.1$  and  $-5.0$ .

The multi variable correlation given in Eq. (1) not only establishes a link between the  $\gamma$ -ray prompt and the afterglow, but it may carry valuable information on the jet opening angle  $\theta_j$ . In the context of the fireball uniform jet model, this angle (supposed to be the same in the prompt and in the afterglow) is related to  $t_{\text{break}}$ , the achromatic break time of the afterglow light curve (Rhoads 1997; Sari, Piran & Halpern 1999). Depending on the circumstellar medium distribution, two models have been proposed. For the homogeneous medium (HM) with number density  $n$ ,

$$\theta_j = 0.161 (t_{\text{break}})^{3/8} \left( \frac{n \eta_{\gamma}}{E_{\text{iso}}} \right)^{1/8} \text{ (HM)}. \quad (2)$$

For a wind medium (WM) with a density profile  $n(r) = 5 \times 10^{11} A r^{-2} \text{ g cm}^{-2}$  (here  $A = 1$  corresponds to the mass loss rate due to a wind of  $\dot{M}_{\text{w}} = 10^{-5} M_{\odot} \text{ yr}^{-1}$  and a wind velocity  $v_{\text{w}} = 10^3 \text{ km s}^{-1}$ ), we have

$$\theta_j = 0.202 (t_{\text{break}})^{1/4} \left( \frac{A \eta_{\gamma}}{E_{\text{iso}}} \right)^{1/4} \text{ (WM)}, \quad (3)$$

where  $\theta_j$  is expressed in radians and  $\eta_{\gamma}$  is the efficiency of the emission, i.e. the fraction of the kinetic energy of the fireball which is emitted in the prompt  $\gamma$ -ray phase. Such estimate of  $\theta_j$  implies the knowledge of  $z$  and of the luminosity distance.

Interestingly enough, by introducing the found multi variable correlation Eq. (1) in Eqs. (2) and (3), one may express  $\theta_j$  in terms of prompt observables. Thus, we obtain approximately that:

$$\theta_j^2 \propto \frac{E_{\text{pk}}^{3/2}}{E_{\text{iso}}} \text{ (HM)}; \quad \theta_j^2 \propto \frac{E_{\text{pk}}}{E_{\text{iso}}} \text{ (WM)}. \quad (4)$$

Defining the collimation corrected energy approximately as  $E_{\gamma} = E_{\text{iso}} \theta_j^2$ , Eqs. (4) lead to

$$E_{\gamma} \propto E_{\text{pk}}^{3/2} \text{ (HM)}; \quad E_{\gamma} \propto E_{\text{pk}} \text{ (WM)}. \quad (5)$$

These relations were extensively discussed by GGL2004 and Nava et al. (2006). Finally, if we identify  $E_{\gamma}/E_{\text{pk}}$  with the total number of photons  $N_{\gamma}$  emitted by the prompt, then an interesting conclusion follows (Nava et al. 2006) :

$$N_{\gamma} \propto E_{\text{pk}}^{1/2} \text{ (HM)}; \quad N_{\gamma} = \text{const} \sim 10^{57} \text{ (WM)}. \quad (6)$$

In §7 we will use these results to compare the  $E_{\text{iso}}-E_{\text{pk}}-t_{\text{break}}$

GRB	$\alpha$	$\beta$	fluence	range	ref	peak flux	range	ref
970228	-1.54±0.08	-2.5±0.4	(1.1±0.1)e-5	40-700	1	(3.7±0.8)e-6	40-700	4
970828	-0.70±0.08	-2.1±0.4	(9.6±0.9)e-5	20-2000	2	(5.9±0.3)e-6	30-10 <sup>4</sup>	10
971214	-0.76±0.10	-2.7±1.1	(8.8±0.9)e-6	40-700	1	(6.8±0.7)e-7	40-700	4
980703	-1.31±0.14	-2.39±0.26	(2.3±0.2)e-5	20-2000	2	(1.6±0.2)e-6	50-300	2
990123	-0.89±0.08	-2.45±0.97	(3.0±0.4)e-4	40-700	3	(1.7±0.5)e-5	40-700	4
990506	-1.37±0.15	-2.15±0.38	(1.9±0.2)e-4	20-2000	1	[18.6±0.1]	50-300	11
990510	-1.23±0.05	-2.7±0.4	(1.9±0.2)e-5	40-700	3	(2.5±0.2)e-6	40-700	4
990705	-1.05±0.21	-2.2±0.1	(7.5±0.8)e-5	40-700	3	(3.7±0.1)e-6	40-700	4
990712	-1.88±0.07	-2.48±0.56	(6.5±0.3)e-6	40-700	3	[4.1±0.3]	40-700	12
991216	-1.23±0.13	-2.18±0.39	(1.9±0.2)e-4	20-2000	2	[67.5±0.2]	50-300	11
000131	-0.69±0.08	-2.07±0.37	(4.2±0.4)e-5	20-2000	1	[7.89±0.08]	50-300	13
000911	-1.11±0.12	-2.3±0.4	(2.2±0.2)e-4	15-8000	1	(2.0±0.2)e-5	15-8000	14
011211	-0.84±0.09	...	...	...	4	(5.0±1.0)e-8	40-700	15
020124	-0.87±0.17	-2.7±0.5	[166±13]	2-400	5,6	[9.4±1.8]	2-400	5
020813	-0.9±0.1	...	[1325±23]	2-400	5	[32.3±2.1]	2-400	5
021211	-0.86±0.09	-2.23±0.20	[93±3]	2-400	5	[30±2]	2-400	5
030226	-0.83±0.16	-2.3	[114±11]	2-400	5	[2.7±0.6]	2-400	5
030328	-1.14±0.03	-2.2±0.3	[751±12]	2-400	5	[11.6±0.9]	2-400	5
030329	-1.26±0.02	-2.28±0.06	[4963±42]	2-400	5	[451±25]	2-400	5
030429	-1.12±0.24	...	[40±5]	2-400	5	[3.8±0.8]	2-400	5
040924	-1.17±0.05	...	(2.7±0.1)e-6	20-500	7,8	(2.6±0.3)e-6	20-500	0
041006	-1.4±0.1	...	(2.0±0.2)e-5	25-100	7	(1.0±0.1)e-6	25-100	0
050525	0.00±0.12	-2.3±0.1	(2.01±0.05)e-5	15-350	9	[47.7±1.2]	15-350	9
980425	-1.0±0.3	-2.1±0.1	(3.8±0.4)e-6	20-2000	16	[0.4±0.1]	50-300	17
990712	-1.88±0.07	-2.48±0.56	(6.5±0.3)e-6	40-700	1	[4.1±0.3]	40-700	1
010921	-1.49±0.16	-2.3	(1.8±0.1)e-5	2-400	5	[40±4]	2-400	5
031203	-1.63±0.1	...	(2.0±0.4)e-6	20-200	18	(2.4±0.2)e-7	20-200	18

**Table 2.**  $\alpha$  and  $\beta$  represent the photon spectral index of the model spectrum. The fluence is given in units of erg cm<sup>-2</sup> (round brackets) or in units of photon cm<sup>-2</sup> (square brackets). The peak flux is given in units of erg cm<sup>-2</sup> s<sup>-1</sup> (round brackets) or photon cm<sup>-2</sup> s<sup>-1</sup> (square brackets). The energy range of the fluence and peak flux is expressed in units of keV. References: (0) This paper; (1) Ghirlanda et al. 2004a and references therein; (2) Jimenez et al. 2001; (3) Amati et al. 2002; (4) Amati et al. 2004; (5) Sakamoto et al. 2005; (6) Atteia et al. 2005; (7) <http://space.mit.edu/HETE/Bursts>; (8) Golenetskii et al. 2004; (9) Blustin et al. 2005; (10) Yonetoku et al. 2004; (11) The BATSE catalogue (Paciesas et al. 1999); (12) Frontera et al. 2001; (13) Andersen et al. 2000; (14) Price et al. 2002; (15) Piro et al. 2005; (16) Yamazaki et al. 2003; (17) Paciesas et al. 1999; (18) Sazonov et al. 2004.

or Ghirlanda correlation with the new one we will introduce in §5.

#### 4 CHARACTERIZING THE VARIABILITY OF THE PROMPT EMISSION

The starting point, as mentioned in the Introduction, are the  $L_{\text{iso}}-E_{\text{pk}}$  or the  $E_{\text{iso}}-E_{\text{pk}}$  correlations. Our aim is to see if the introduction of more prompt variables can produce significantly tighter correlations than these ones. Among the most relevant information from the  $\gamma$ -ray prompt emission is the lightcurve.

The variability  $V$ , a quantity that estimates the “spikiness” of the lightcurve (see for details Fenimore & Ramirez-Ruiz 2000), offers a way to partially quantify the information contained in the light curves.

Here we introduce another variability indicator making use of the fluence  $F$  to the peak flux  $P$  ratio. Such ratio gives a time, which compared with a burst timescale provides a further characterization of the lightcurve pattern variability. We calculate the  $F/P$  ratio using the *bolometric corrected* quantities (in the range of 1 – 10<sup>4</sup> keV). Using the prompt

“high-signal” timescale,  $T_{0.45}^{\text{obs}}$  (see next subsection) we define, in the GRB rest frame

$$\Phi = \frac{L_{\text{iso}} T_{0.45}}{E_{\text{iso}}}, \quad (7)$$

where  $T_{0.45} = T_{0.45}^{\text{obs}}/(1+z)$ .  $\Phi$  is a scalar with a clear meaning in the observer frame, the GRB rest frame, and the fireball comoving frame. If one multiplies the numerator and denominator of the right term by  $\theta_j^2/E_{\text{pk}}$ , then  $\Phi$  reveals itself as the ratio of the number of photons emitted during the “high-signal” regime to the total number of emitted photons, which is particularly interesting in the comoving frame. A further advantage is that  $\Phi$  may be derived from observables easy to handle.

##### 4.1 Definition of variability

The definition of the variability  $V$  requires the estimate of a smoothing time scale,  $T_{0.45}^{\text{obs}}$ , that, following R2001, we assume to be *the time spanned by the brightest 45% of the total counts above the background*. In practice, we estimate from the light curve the fraction of counts and the total time when the signal exceeds a given threshold. We identify the threshold when this fraction is 0.45, and we calculate the total time during which the signal exceeds this threshold. The

GRB	class	$E_{pk}$	ref	$E_{iso}$	ref	$L_{iso}/E_{iso}$	Var	ref
970228	1	195±64	1	(1.60±0.12)e52	1	(5.7±1.3)e-1	0.08±0.05	8
970828	1	583±116	2	(2.96±0.35)e53	1	(8.5±2.4)e-2	0.10±0.01	8
971214	1	685±133	1	(2.11±0.24)e53	1	(34.2±5.0)e-2	0.087±0.004	0
980703	1	502±100	2	(6.9±0.8)e52	1	(30.3±6.1)e-2	0.064±0.003	0
990123	1	2030±160	3	(2.4±0.3)e54	1	(14.7±4.8)e-2	0.129±0.001	0
990506	1	653±130	1	(9.5±1.1)e53	1	(4.4±1.3)e-2	0.326±0.001	0
990510	1	423±42	3	(1.8±0.2)e53	1	(34.0±4.6)e-2	0.229±0.002	0
990705	1	348±28	3	(1.82±0.23)e53	1	(9.1±1.0)e-2	0.15±0.05	8
990712	1	93±15	3	(6.7±1.3)e51	1	(11.1±1.9)e-2	...	
991216	1	641±128	2	(6.75±0.81)e53	1	(16.8±5.2)e-2	0.124±0.001	0
000131	1	714±142	1	(1.84±0.22)e54	1	(7.7±2.9)e-2	0.11±0.01	8
000911	1	1190±238	1	(8.8±1.0)e53	1	(18.7±2.5)e-2	0.077±0.034	9
011211		186±24	4	(5.4±0.6)e52	1	...	...	
020124	1	390±113	5	(2.15±0.73)e53	0	(23.8±4.9)e-2	0.29±0.04	0
020813	2	478±95	6	(4.7±0.3)e53	0	(54.8±3.7)e-3	0.247±0.004	0
021211	1	92±14	7	(1.10±0.13)e52	1	(64.8±4.8)e-2	0.006±0.004	0
030226	2	289±63	7	(1.20±0.13)e53	1	(7.1±1.7)e-2	0.08±0.04	0
030328	1	318±34	7	(2.80±0.33)e53	1	(38.9±3.1)e-3	0.052±0.006	0
030329	1	79±3	7	(1.8±0.2)e52	1	(10.6±0.6)e-2	0.104±0.002	0
030429	2	128±26	7	(2.19±0.26)e52	1	(34.7±8.5)e-2	...	
040924	2	125±12	10	(7.3±0.8)e51	0	(18.6±2.9)e-1	0.007±0.001	0
041006	2	109±22	11	(7.1±0.8)e52	0	(8.6±1.2)e-2	0.082±0.003	0
050525	3	127±6	12	(3.5±0.5)e52	0	(24.7±1.6)e-2	0.099±0.001	0
980425		119±24	1	(1.6±0.2)e48	1	(4.18±1.19)e-2	0.0055±0.005	0
990712		93±16	1	(6.72±1.29)e51	1	(1.11±0.19)e-1	0.042±0.017	0
010921		154±30	1	(1.5±0.1)e52	0	(8.30±1.00)e-2	0.010±0.009	0
031203		>210	13	(1.0±0.4)e50	0	(1.33±0.30)e-1	0.1±0.01	0

**Table 3.** The peak energy  $E_{pk}$  and the bolometric isotropic equivalent energy  $E_{iso}$  are expressed in units of keV and erg, respectively.  $E_{iso}$  and  $L_{iso}$  are calculated in the 1–10<sup>4</sup> keV rest frame energy band. The Variability (Var) is calculated as described in the text (§4). References: (0) This paper (1) Ghirlanda et al 2004a (references therein); (2) Jimenez et al. 2001; (3) Amati et al. 2002; (4) Amati et al. 2004; (5) Atteia et al. 2005; (6) Barraud et al. 2003; (7) Sakamoto et al. 2005; (8) Reichart et al. 2001; (9) Guidorzi et al. 2005; (10) Golenetskii et al. 2004; (11) <http://space.mit.edu/HETE/Bursts>; (12) Blustin et al. 2005; (13) Sazonov et al. 2004;

assumed energy range is 50 – 300 keV at rest. We use the recipe proposed by R2001 to pass from the observed energy range to the assumed rest one. Finally, we use the lightcurve time binning of *HETE-II*, 164–ms. Though for most of the *BATSE* GRBs the time bin is 64–ms, we preferred to take the larger *HETE-II* time bin for uniformity. In Table 1 we report the  $T_{0.45}^{obs}$  calculated by us from the publicly available lightcurves. In the few cases when the lightcurves were not available, we have used the time scales  $T_{0.45}^{obs}$  reported in R2001 and, for one event (see below), in Guidorzi et al. (2005).

The  $V$  parameter decreases systematically with the S/N ratio. In order to handle a quantity characterizing the signal it is necessary to disentangle the noise contribution. To this purpose R2001 suggested an analytic approximation. We introduce here an alternative method, with the aim to reduce the uncertainty on the variability noise correction avoiding any approximation. Our method is especially useful for data with a low S/N ratio. Based on the assumption that the photon shot noise obeys a Poissonian distribution, we use a Monte Carlo approach to simulate the noise contribution to the variability.

The basics of our approach is as follows. Given a noiseless signal (*zero order*) with an *intrinsic variability*, we can introduce a *first order* realization of the signal by distorting it with its own Poisson noise. The *first order variability* will be different from the *intrinsic variability*. Then we construct

a *second order* realization of the signal distorting the previous *first order* realization with its own Poisson noise. This *second order* realization will have a new variability. *Higher order* realizations may be carried out up to a fixed number. The sequence of realizations may be randomly repeated and the average behavior and scatter of the variability sequences may be obtained. A simple statistical analysis allows to recover the *intrinsic variability* with some uncertainty from the higher (first, second,...) order realizations. Numerical experiments up to the third order realizations have been carried out successfully on artificial signals. We have found that the simple linear extrapolation  $V_0 = 2V_1 - V_2$  is enough to obtain a reasonable zero order estimate (here the index identifies the order). In the case of a real signal, the *zero order* signal is unknown while its *intrinsic variability* is the result we are looking for. Actually we have just a *first order* realization with its intrinsic Poisson noise. Starting from here we apply the previous scheme building several times the *second order* realizations. The final result is the *intrinsic variability* with its uncertainty.

We have taken some care to test our method using a real GRB light curve. To this aim, we have assumed that the observed light curve is a pure zero order signal (i.e. ignore any Poisson noise and call  $V_0$  the variability of this light curve). Then we have distorted this signal once with a Poisson noise obtaining a first order realisation ( $\tilde{V}_1$ ), and finally on this one we have applied our method (i.e. derive  $\tilde{V}_2$  by a Monte

Carlo method, extrapolate back and estimate the average  $\tilde{V}_0$  and its error). The result may be compared now with the variability of the “zero” order signal  $V_0$ . In the case of the rather noisy GRB 971214 light curve,  $V_0 = 0.1169$  lies inside the obtained  $\tilde{V}_0 = 0.116 \pm 0.004$  ( $1\sigma$  error), while for the high signal GRB 991216 light curve we have  $V_0 = 0.1438$ , which is consistent with  $\tilde{V}_0 = 0.1445 \pm 0.0010$ .

In principle our variability estimate follows a different procedure from the original method proposed by R2001, therefore a comparison between the two methods is desirable. We have used the GRBs of our sample in common with the R2001 sample to compare the values of  $T_{0.45}^{\text{obs}}$  and  $V$ . From the results given in Table 1 and Table 3 it can be seen that our method gives  $T_{0.45}^{\text{obs}}$  and  $V$  in general good agreement with those published by R2001. The only difference is a smaller uncertainty in our estimate of  $V$ . The fact that our results agree with R2001 justifies the inclusion in our sample of four GRBs whose  $V$  and  $T_{0.45}^{\text{obs}}$  have been estimated by R2001 only.

In a recent paper, Guidorzi et al. (2005) have presented new calculations of  $V$  for a sample of 32 GRBs. For some GRBs in common with our sample, the processed lightcurves used by these authors could differ from the ones used by us. Besides, for the *BeppoSAX*/WFC events they apply two further “instrumental” corrections in the calculation of  $V$  that we did not apply because of the lack of information. According to the authors, these corrections affect  $V$  significantly only for relatively short GRBs exhibiting sharp intense pulses. On the other hand, our calculation of  $V$  and its uncertainty includes a new method to treat the noise correction that improves the results especially for data with low S/N ratios, while Guidorzi et al. (2005) use the same analytical approach of R2001. We have compared  $T_{0.45}^{\text{obs}}$  and  $V$  for the 5 GRBs in common with Guidorzi et al. (2005). Some discrepancies have been found. Therefore, for reasons of homogeneity, we have included in our sample the measured  $T_{0.45}^{\text{obs}}$  and  $V$  from Guidorzi et al. (2005) only for one event, GRB 000911.

## 5 A NEW TIGHT CORRELATION

Our aim is to find correlations among prompt  $\gamma$ -ray quantities alone, with the smallest scatter. For example, we would like to explore the possibility to improve the  $L_{\text{iso}}-E_{\text{pk}}$  ( $E_{\text{iso}}-E_{\text{pk}}$ ) “power” (“energy”) correlations by introducing the prompt emission variables  $T_{0.45}$ ,  $V$ , and  $\Phi$ , which partially characterize the  $\gamma$ -ray light curve (see §4). We remark that in our statistical analysis we take into account the uncertainties of the data. Notice that the variables always refer to the GRB rest frame. Our main criterion to judge about the goodness of the fit will be the value of the reduced  $\chi^2$ .

Among other combinations, we look for a multi variable linear correlation of  $\text{Log}\Phi$  as a function of a combination of  $\text{Log}E_{\text{pk}}$ ,  $\text{Log}E_{\text{iso}}$ ,  $\text{Log}T_{0.45}$   $\text{Log}V$  ( $L_{\text{iso}}$  is already contained in the variable  $\Phi$ ). This approach also allows us to explore whether the lightcurve variables,  $\Phi$  and  $V$ , are correlated among them or not. Only the 15 high-quality (class 1) events with accurately measured variability  $V$  are used in the regression analysis. The best fit is:

$$\frac{L_{\text{iso}} T_{0.45}}{E_{\text{iso}}} = 10^{-0.32 \pm 0.03} \left( \frac{E_{\text{pk}}}{10^{2.38} \text{ keV}} \right)^{1.51 \pm 0.25} \times$$

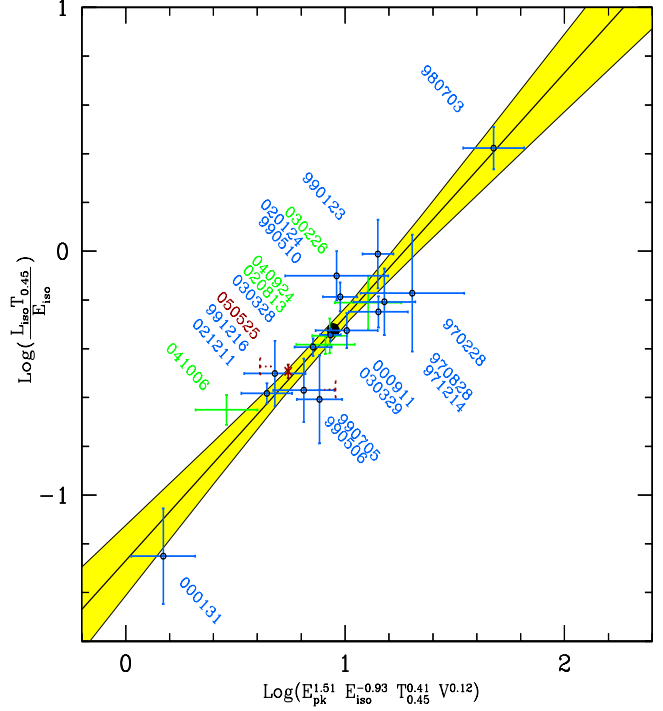


**Figure 2.** Multi variable linear regression analysis based on the 15 GRBs of class 1 (open circles). The best fit (solid line) corresponds to Eq. 8 and the shaded region is the  $1\sigma$  uncertainty of this equation. The latter is computed in the barycenter of the data points (solid black point). Color codes have the same meaning as in Fig. 1.

$$\left( \frac{E_{\text{iso}}}{10^{2.95} \text{ erg}} \right)^{-0.93 \pm 0.16} \left( \frac{T_{0.45}}{10^{0.53} \text{ s}} \right)^{0.41 \pm 0.10} \times \left( \frac{V}{10^{-1.06}} \right)^{0.12 \pm 0.10}, \quad (8)$$

with  $\chi_r^2=0.62$  (for 10 dof). Fig. 2 shows the data and the best fit given by Eq. (8) in a two dimensional diagram. The uncertainties in the data, showed with error bars, were taken into account in the regression analysis. The (yellow) shaded area corresponds to the  $1\sigma$  confidence interval of the regression line (Eq.8). The data used for the fitting are marked with open circles. The class 2 events and GRB 050525 are also plotted in Fig. 2, although they were not used in the fit.

From Eq. (8) one sees that  $\Phi$  is correlated with  $V$  very weakly, since its exponent is almost consistent with zero. We also note that  $E_{\text{iso}}$  is not an important variable in the correlation represented by Eq. (8), because it appears with almost the same power on both sides of this equation. Therefore, the significant variables are  $L_{\text{iso}}$ ,  $E_{\text{pk}}$  and  $T_{0.45}$ . In a first approximation, from Eq. (8) we may infer that  $L_{\text{iso}} \propto E_{\text{pk}}^{1.5} T_{0.45}^{-0.5}$ .

We therefore proceed to perform the multi variable regression analysis (taking into account the uncertainties) for  $\text{Log}L_{\text{iso}}$  as a function of  $\text{Log}E_{\text{pk}}$  and  $\text{Log}T_{0.45}$ . For the same events used previously, we obtain a fit with  $\chi_r^2=0.67$  (for 13 dof) that, compared with the  $\chi_r^2=0.62$  of the correlation given by Eq. (8), implies again that the variables  $V$  and  $E_{\text{iso}}$

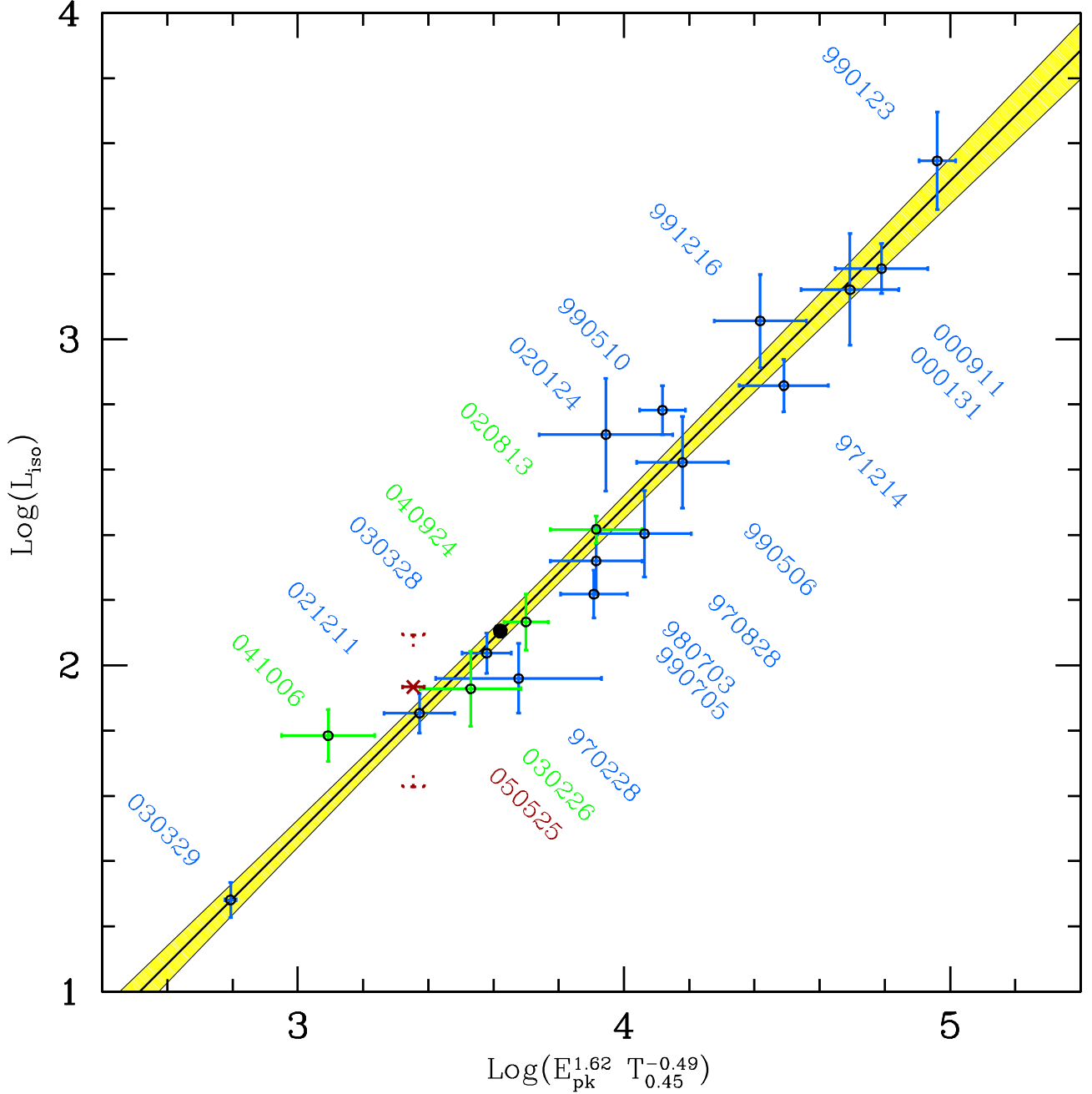


**Figure 3.** Multi variable linear regression analysis based on 19 GRBs (class 1 [blue crosses] and class 2 [green crosses] events in Tab. 3). The best fit, corresponding to Eq. 9, and its  $1\sigma$  uncertainty (computed in the barycenter of the data points - solid black point) are represented by the solid line and by the shaded (yellow) region, respectively. using the same convention of Fig. 1.

are redundant for the correlation in Eq. 8. In order to use as many data as possible, we also performed the regression analysis including 4 events of class 2 (GRB 030429 lacks a measure of  $T_{0.45}^{\text{obs}}$ ), for a total of 19 events. The best fit is:

$$L_{\text{iso}} = 10^{52.11 \pm 0.03} \left( \frac{E_{\text{pk}}}{10^{2.37} \text{ keV}} \right)^{1.62 \pm 0.08} \times \left( \frac{T_{0.45}}{10^{0.46} \text{ s}} \right)^{-0.49 \pm 0.07} \text{ erg s}^{-1} \quad (9)$$

with  $\chi_r^2=0.70$  (for 16 dof). Fig. 3 shows the data, the best fit and its  $1\sigma$  confidence interval (shaded area) in a two dimensional diagram. GRB 050525 was not used for the regression analysis but it is plotted in Fig. 3.

The correlation  $L_{\text{iso}}-E_{\text{pk}}-T_{0.45}$  is very tight, which can be appreciated from Fig. 4, where we show the scatter (taken as the orthogonal distance of the data points to the best fit line). Fitting the scatter distribution with a Gaussian



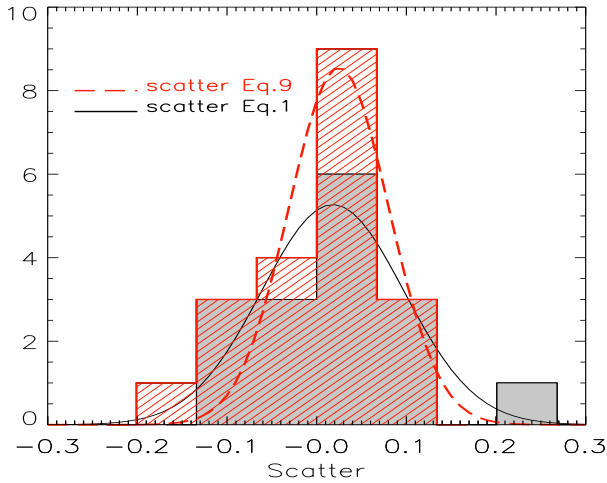


**Figure 4.** Histogram of the (logarithmic) scatter of the data points around the best fit of Eq. 9 (light gray) and Eq. 1 (darker gray). We superpose the two Gaussian fits.

yields a (logarithmic) dispersion  $\sigma = 0.06$ , smaller than the corresponding dispersion of points around the correlation described by Eq. 1 (a Gaussian yields  $\sigma = 0.08$ ).

The correlation of Eq. 9 is a significant improvement (i.e. it has a smaller scatter) of the  $L_{\text{iso}}-E_{\text{pk}}$  correlation found by Yonetoku et al. (2004). In fact, for the updated version of the Yonetoku correlation, Ghirlanda et al. (2005) found a  $1\sigma$  dispersion of 0.25. We have explored other multi variable correlations and the one given by Eq. (9) was indeed the tightest with significant variables.

The fact that  $\chi_r^2$  is smaller than 1 might be a consequence of an overestimate in the observational uncertainties of the data as well as of unaccounted correlation among the variable errors. Indeed, we have assumed that the errors in the variables are uncorrelated (§2). If the errors instead have some degree of correlation among them (which is very likely), then we are overestimating their contribution to  $\chi_r^2$ .

Fig. 3 shows the main result of this paper, namely the existence of a very tight empirical relation among the peak luminosity of the GRB ( $L_{\text{iso}}$ ) and the prompt  $\gamma$ -ray quantities  $E_{\text{pk}}$  and  $T_{0.45}$ . This relation is as tight as the  $E_{\text{iso}}-E_{\text{pk}}-t_{\text{break}}$  one (see §3).

In Fig. 5 we display the available GRB light-curves following the same sequence of data points (from top-right to bottom-left) plotted in Fig. 3. The different patterns appear mixed, and there is no hint of any sequence.

We have also performed a linear regression analysis to find the best fit in our sample for  $L_{\text{iso}}-E_{\text{pk}}-T_{90}$ , i.e. using the variable  $T_{90}$  at rest instead of  $T_{0.45}$ . The obtained multivariable correlation is similar to the one given by Eq. (9) but with a significant larger scatter.

### 5.1 The lowest-luminosity GRBs in the $L_{\text{iso}}-E_{\text{pk}}-T_{0.45}$ diagram

There are four GRBs that were not included in our sample: GRB 980425 (a rather peculiar burst), GRB 990712 and GRB 010921 (they were not included in our sample

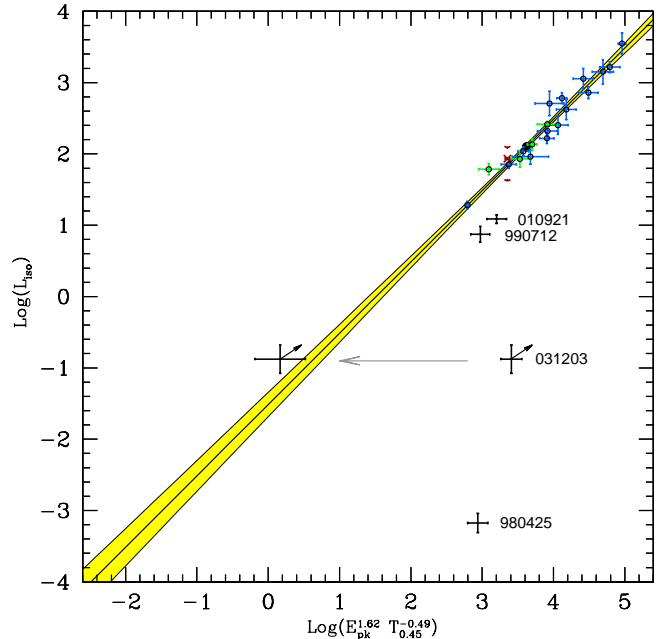


**Figure 6.** Similar to Fig. 3 but including the “outliers” GRB 980425, GRB 990712, GRB 010921 and GRB 031203. If the X-ray  $E_{\text{pk}}$  reported by Watson et al. (2006) is used, then the position of GRB 031203 (lower limit calculated for  $E_{\text{pk}} = 200 \pm 40 \text{ keV}$ ) shifts close to the correlation given by Eq. 9.

because they have a too uncertain determination of  $V$ ), and GRB 031203 (another peculiar burst, as GRB 980425). All these bursts are low luminosity events. It is interesting to see a posteriori where they lie in the  $\text{Log} L_{\text{iso}}$  vs  $\text{Log}(E_{\text{pk}}^{1.62} T_{0.45}^{-0.49})$  plot.

Fig. 6 shows the same correlation of Fig. 3 but we include here these four low luminosity events. Curiously enough, they break the main correlation at its lowest end, below  $L_{\text{iso}} \approx 10^{51.2} \text{ erg s}^{-1}$ , giving rise to a kind of low luminosity branch (determined mainly by a minimum value of  $E_{\text{pk}}$  and, at a less extent, by a maximum value of  $T_{0.45}$ ).

In a recent paper, Watson et al. (2006) have shown that GRB 031203 might have a soft X-ray spectral component, at  $\sim 2 \text{ keV}$ . This component carries a fluence which is even higher than the  $\gamma$ -ray one. Therefore it is this soft component which can determine the peak energy  $E_{\text{pk}}$ .

If we use  $E_{\text{pk}}$  of the X-ray component reported in Watson et al. (2006), then the position of GRB 031203 in Fig. 6 shifts to the left as indicated by the arrow in Fig. 6. In this case GRB 031203 lies close to the multi variable correlation given by Eq. (9). Furthermore, the reported spectra of GRB 990712 and GRB 010921 (Amati et al. (2002) and Sakamoto et al. (2005), respectively), seems peculiar: in the case of GRB 990712 the spectrum is rather flat in  $\nu F(\nu)$ , making the determination of  $E_{\text{pk}}$  uncertain, and in the case of GRB 010921 the spectrum has some local bumps at energies lower than the reported  $E_{\text{pk}}$  (Barraud et al. 2003). It is then possible that also these two sources lie very close to the main correlation shown in Fig. 6.

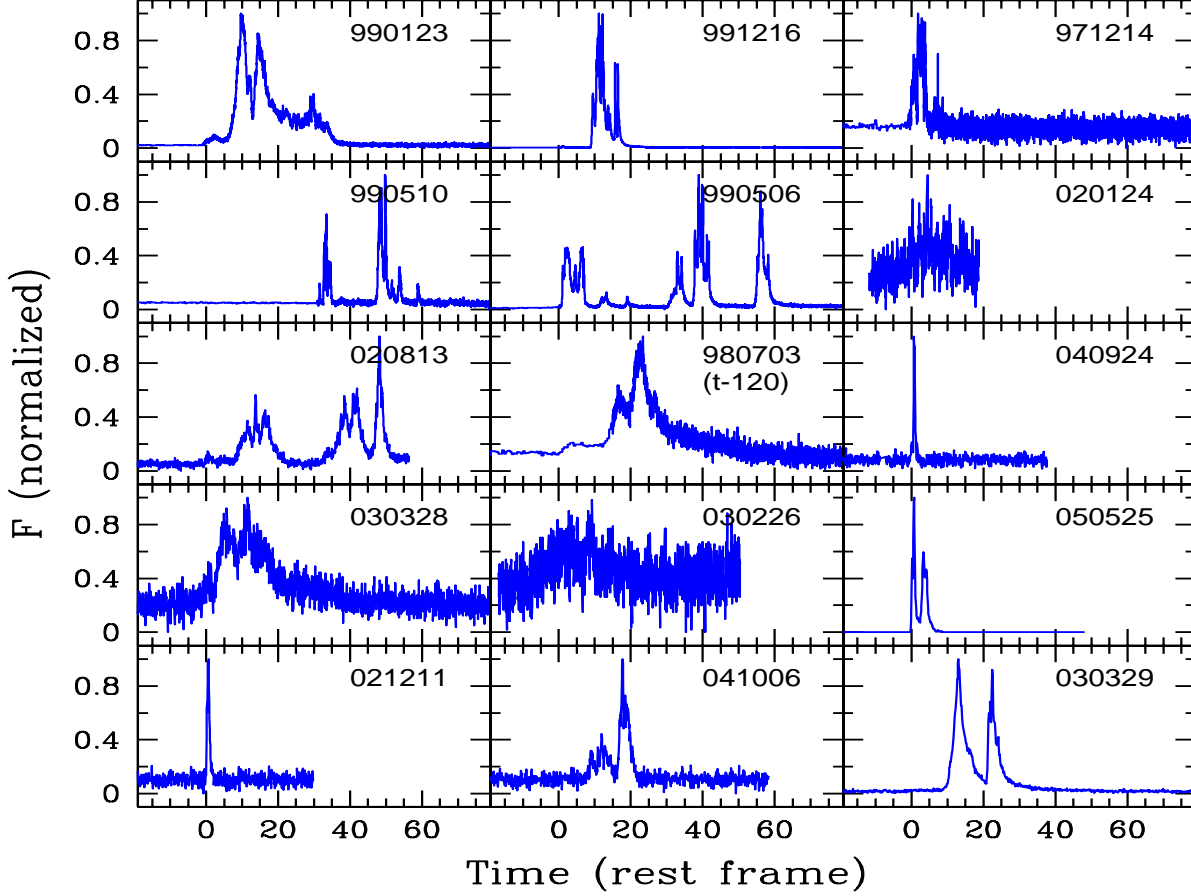


**Figure 5.** The sequence of the available GRB light curves of our sample. The order follows the distribution of GRBs along the sequence of Fig. 3 from top-right to bottom-left.

## 6 THE $L_{\text{iso}}-E_{\text{pk}}-T_{0.45}$ CORRELATION AS A REDSHIFT INDICATOR

The tightness of the multi variable  $L_{\text{iso}}-E_{\text{pk}}-T_{0.45}$  correlation (see Fig. 4) encourages us to use it as new distance (redshift) indicator for GRBs with no measured redshifts. In fact, the great advantage of this correlation is that involves only prompt emission quantities which can be easily derived from the  $\gamma$ -ray lightcurve and spectra of GRBs with unknown  $z$ .

This way, we could have a statistically significant GRB luminosity-redshift diagram to infer the GRB luminosity function and the GRB formation rate history (e.g., Schaefer, Deng & Band 2001; Lloyd-Ronning, Fryer & Ramirez-Ruiz 2002; Firmani et al. 2004; Yonetoku et al. 2004).

The bolometric corrected peak flux, in the observer frame, is connected to the bolometric corrected isotropic luminosity  $L_{\text{iso}}$  by:

$$P = \frac{L_{\text{iso}}}{4\pi D_L^2(z)} \quad (10)$$

where  $D_L(z)$  is the luminosity distance. The cosmologi-

cal redshift and time dilation effect impose that  $E_{\text{pk}} = E_{\text{pk}}^{\text{obs}}(1+z)$  and  $T_{0.45} = T_{0.45}^{\text{obs}}/(1+z)$ . However, the use of  $T_{0.45}^{\text{obs}}$  needs a particular care. In fact, as mentioned in §2.1,  $T_{0.45}^{\text{obs}}$  (and consequently  $T_{0.45}$ ) is calculated from a light curve defined over an energy range which is fixed in the rest frame of the GRB (see also R2001). Using the approximation given by R2001 that takes into account the narrowing of the light curve temporal substructures at higher energies, we obtain  $\tilde{T}_{0.45}^{\text{obs}} = T_{0.45}^{\text{obs}}/(1+z)^{0.4}$ , where  $\tilde{T}_{0.45}^{\text{obs}}$  is measured in the same energy range but defined now in the observer frame. It follows that  $T_{0.45}$  measured in the source rest frame is  $T_{0.45} = \tilde{T}_{0.45}^{\text{obs}}/(1+z)^{0.6}$ .

Once we know how the rest frame quantities  $L_{\text{iso}}$ ,  $E_{\text{pk}}$  and  $T_{0.45}$  transform with the redshift  $z$ , we may express the  $L_{\text{iso}}-E_{\text{pk}}-T_{0.45}$  relation (Eq. 9) in terms of the observer frame equivalent quantities:

$$P4\pi D_L^2(z) = 10^{52.11 \pm 0.03} \left[ \frac{E_{\text{pk}}^{\text{obs}}(1+z)}{10^{2.37} \text{ keV}} \right]^{1.62 \pm 0.08} \times \left[ \frac{\tilde{T}_{0.45}^{\text{obs}}}{(1+z)^{0.6} 10^{0.46} \text{ s}} \right]^{-0.49 \pm 0.07} \text{ erg s}^{-1} \quad (11)$$

GRB	$z$	$\bar{z}$	$\Delta z/z$
970228	0.695	0.940	0.353
970828	0.958	1.212	0.265
971214	3.420	4.801	0.404
980703	0.966	1.104	0.142
990123	1.600	1.358	-0.151
990506	1.307	1.418	0.085
990510	1.619	1.210	-0.253
990705	0.843	1.109	0.315
991216	1.020	0.823	-0.193
000131	4.500	4.957	0.102
000911	1.058	1.173	0.108
020124	3.198	1.797	-0.438
020813	1.255	1.235	-0.016
021211	1.010	1.032	0.022
030226	1.986	2.398	0.208
030328	1.520	1.613	0.061
030329	0.169	0.170	0.008
040924	0.859	0.941	0.095
041006	0.716	0.547	-0.236

**Table 4.** Spectroscopically measured redshifts ( $z$ ) and pseudo-redshifts ( $\bar{z}$ ) derived according to the procedure described in Sec. 7 for 20 GRBs of our sample.  $\Delta z/z$  represents the uncertainty of the derived pseudo-redshifts.

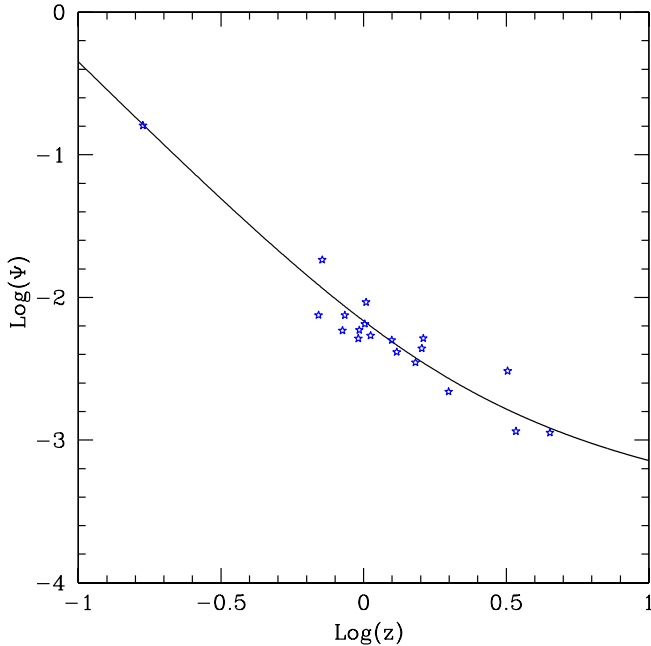


**Figure 7.** The line shows the pseudoreshift given by Eq. 15, while the data show the observed redshifts for the 19 GRBs of the sample of Fig. 3.

We indicate the ratio between observer frame measured quantities as  $\Psi$  and we isolate the redshift dependences in the term  $f(z)$ :

$$f(z) = \frac{(1+z)^{1.91}}{4\pi D_L^2} \quad (12)$$

$$\Psi \equiv \frac{P(\tilde{T}_{0.45}^{\text{obs}})^{0.49}}{E_{\text{pk}}^{\text{obs}1.62}}, \quad (13)$$

so that Eq. 11 reduces to:

$$f(z) = C\Psi, \quad (14)$$

where  $C$  is fixed to  $10^{6.48}$  such that  $D_L$ ,  $P$ ,  $E_{\text{pk}}^{\text{obs}}$ , and  $\tilde{T}_{0.45}^{\text{obs}}$  are expressed in unities of Gpc, erg cm<sup>-2</sup> s<sup>-1</sup>, keV and sec, respectively.

For the  $\Lambda$ CDM cosmological model assumed in this paper, the inversion of Eq. (14) allows us to estimate the pseudo-redshift  $\bar{z}$  of a given GRB whose  $P$ ,  $E_{\text{pk}}^{\text{obs}}$ , and  $\tilde{T}_{0.45}^{\text{obs}}$  have been measured from the prompt emission  $\gamma$ -ray light curve solely:

$$\bar{z} = f^{-1}(C\Psi). \quad (15)$$

In Fig. 7 we plot Eq. (14) as  $\text{Log}\Psi$  vs.  $\text{Log}(z)$  (solid line). The sample of GRBs used to derive the  $L_{\text{iso}}-E_{\text{pk}}-T_{0.45}$  correlation are also plotted (stars). The notably small scatter of the data points around the curve is a proof of the reliability of the redshift indicator inferred from the  $L_{\text{iso}}-E_{\text{pk}}-T_{0.45}$  correlation. In Table 5 we give for the 19 GRBs of our sample the spectroscopically measured  $z$ , the pseudo-redshifts  $\bar{z}$  derived from Eq. 15, and the relative uncertainty between these two quantities. We note that the 68% of our pseudo redshifts (i.e. 13 out of 19 sources) are within the 25% of the real value. In Fig. 8 we compare the distribution of the  $\Delta z/z$  values obtained with Eq. 15 with the one found by Atteia (2003). One can see that the our distribution is somewhat narrower, and especially that the central value is closer to zero.

Moreover, as can be inferred from the data reported in Table 4, the relative uncertainty on the derived pseudo-redshifts does not seem to be correlated with the redshifts. This suggests that the  $L_{\text{iso}}-E_{\text{pk}}-T_{0.45}$  correlation can be used to estimate either low and high values of  $z$ .

Finally we note that the  $T_{0.45}^{\text{obs}}$  parameter can be derived from the prompt emission lightcurve straightforwardly. On the other hand, the use of Eq. 15 to estimate  $z$  requires the measure of the GRB peak spectral energy  $E_{\text{pk}}^{\text{obs}}$  from the fit of a broad-band spectrum.

## 7 THEORETICAL IMPLICATIONS AND CHALLENGES

### 7.1 Comparison with other correlations

The most important correlation found in this paper among  $L_{\text{iso}}$ ,  $E_{\text{pk}}$  and  $T_{0.45}$  can be compared with the other tight correlations between the emitted energy or luminosity,  $E_{\text{pk}}$  and  $t_{\text{break}}$ . Consider first the Amati relation between  $E_{\text{iso}}$  and  $E_{\text{pk}}$ . It has a relatively large scatter, which “collapses” when calculating the collimation corrected emitted energy  $E_\gamma$ . In this case, the “collapsing parameter” going from the Amati to the Ghirlanda relation is the jet opening angle, measured by  $t_{\text{break}}$ . If indeed  $\theta_j$  is well measured by  $t_{\text{break}}$ , then the existence of the Ghirlanda relation implies the existence of the phenomenological  $E_{\text{iso}}-E_{\text{pk}}-t_{\text{break}}$  tight relation (Eq. 1) (and vice-versa).

Consider now the Yonetoku relation between  $L_{\text{iso}}$  and  $E_{\text{pk}}$ . As detailed in Ghirlanda et al. (2005), it has a scatter which is comparable to the scatter of the Amati relation.

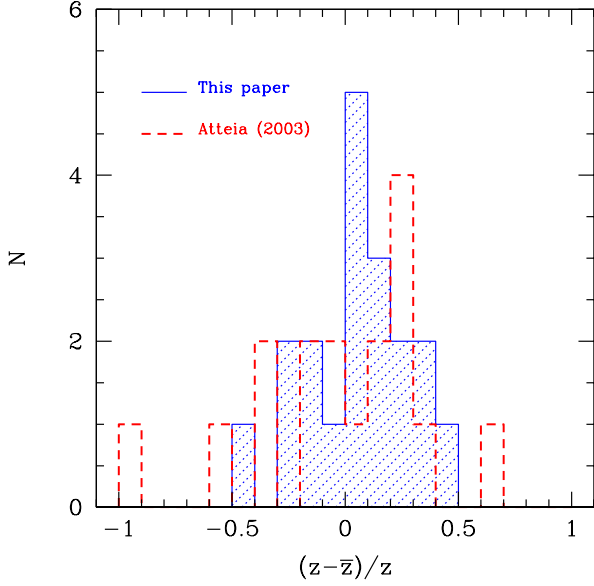


**Figure 8.** Histograms of the values of  $\Delta z/z$  obtained with the method discussed in this paper (hatched, 19 GRBs) and by Atteia (2003, dashed line, 17 GRBs).

But if we now calculate  $L_\gamma$  (correcting for the jet opening angle), then we *do not* find a correlation as tight as the Ghirlanda one. Therefore the “collapsing parameter” which worked for the total energetics does not work for the peak luminosity. The correlation found in this paper demonstrates that a better “collapsing parameter” for the peak luminosity is  $T_{0.45}$ .

From this we can already conclude that  $T_{0.45}$  is *not* equivalent to the jet opening angle: if it were, then both  $T_{0.45}$  and  $\theta_j$  (or  $t_{\text{break}}$ ) should work as collapsing parameters without “caring” if dealing with total prompt energetics or peak luminosities.

Therefore the two tight empirical multi variable correlations  $L_{\text{iso}}-E_{\text{pk}}-T_{0.45}$  (Eq. 9) and  $E_{\text{iso}}-E_{\text{pk}}-t_{\text{break}}$  (Eq. 1) represent two different aspects of the GRB physics.

## 7.2 “Local” versus “global” properties

It is of some interest to make a distinction between *local* and *global* properties of GRBs. If the fireball has a semi-aperture angle  $\theta_j > 1/\Gamma$ , we can see only a portion of the emitting surface (or volume). The peak flux, the fluence and the timescale  $T_{0.45}$  are defined as local quantities since they correspond only to the “observable” surface (or volume). This implies that also  $L_{\text{iso}}$  and  $E_{\text{iso}}$  are basically local quantities. We can then introduce the concept of “local brightness” characterizing the flux emitted by the visible fraction of the fireball. On the other hand, the jet opening angle  $\theta_j$  (and consequently  $t_{\text{break}}$ ) is a global quantity. This implies that  $E_\gamma$  and the Ghirlanda relation are expressions of a global property of GRBs. On the other hand, the  $L_{\text{iso}}-E_{\text{pk}}-T_{0.45}$  relation involves the local brightness (entering in the definition of  $L_{\text{iso}}$ ), which is a local property. Furthermore,  $L_{\text{iso}}$  is an instantaneous quantity, not time integrated (contrary to  $E_{\text{iso}}$  or  $E_\gamma$ ).

We now discuss some implications of the combination

of the  $E_{\text{iso}}-E_{\text{pk}}-t_{\text{break}}$  and the  $L_{\text{iso}}-E_{\text{pk}}-T_{0.45}$  relations. We can divide both sides of Eq. 9 by  $\Phi$  (see Eq. 8) so that  $E_{\text{iso}}$  becomes the dependent variable in Eq. 9 as it is in Eq. 1. A more rigorous result can be obtained by fitting (with the multi variable regression technique)  $\text{Log}E_{\text{iso}}$  as a function of  $\text{Log}E_{\text{pk}}$ ,  $\text{Log}T_{0.45}$  and  $\text{Log}\Phi$ . The best fit, obtained for our sample (including class 1 and 2 GRBs for a total of 19 events), is:

$$E_{\text{iso}} = 10^{52.90 \pm 0.03} \left( \frac{E_{\text{pk}}}{10^{2.36} \text{ keV}} \right)^{1.63 \pm 0.08} \times \left( \frac{T_{0.45}}{10^{0.46} \text{ s}} \right)^{0.51 \pm 0.07} \left( \frac{\Phi}{10^{-0.34}} \right)^{-1.00 \pm 0.15} \text{ erg} \quad (16)$$

with  $\chi_r^2 = 0.64$  (for 15 dof). This multi variable correlation is completely equivalent to that of Eq. (9). By eliminating  $E_{\text{pk}}$  in Eqs. (16) and (1), we can express  $t_{\text{break}}$  as a function of  $\Phi$  and  $T_{0.45}$  (the dependence on  $E_{\text{iso}}$  becomes negligible):

$$t_{\text{break}} \approx 4 \left( \frac{\Phi^2}{T_{0.45}} \right)^{0.6} \text{ days} \quad (17)$$

Eq. 17 establishes a clear connection between prompt emission local quantities ( $\Phi$  and  $T_{0.45}$ ), which are related to the  $\gamma$ -ray lightcurve variability, and an afterglow emission global quantity, i.e.  $t_{\text{break}}$ .

LZ2005 suggested that  $t_{\text{break}}$  could be related to the prompt ( $\gamma$ -ray) emission rather than to the afterglow one.  $t_{\text{break}}$  enters in the Ghirlanda correlation by means of the jet opening angle (see §3), and, as discussed in LZ2005, it raises the question of how a global quantity (i.e.  $\theta_j$ ) conspires with  $E_{\text{iso}}$  to affect  $E_{\text{pk}}$ , which, instead, are both local quantities.

It could be that  $t_{\text{break}}$  is determined by only prompt emission local quantities. This is as also suggested by the reported (Salmonson & Galama (2002)) correlation between the pulse lag of the prompt  $\gamma$ -ray emission and  $t_{\text{break}}$ . This might justify the existence of an empirical correlation between the jet angle (derived from  $t_{\text{break}}$ ) and the local properties  $E_{\text{iso}}$  and  $E_{\text{pk}}$ . Therefore, our finding that  $t_{\text{break}}$  is closely related to the prompt lightcurve quantities  $\Phi$  and  $T_{0.45}$  (Eq. 17) could be the basis of the Ghirlanda and the  $E_{\text{iso}}-E_{\text{pk}}-t_{\text{break}}$  correlations.

## 7.3 The $L_{\text{iso}}-E_{\text{pk}}-T_{0.45}$ correlation in the comoving frame

Another important aspect concerns the transformation of the relation  $L_{\text{iso}}-E_{\text{pk}}-T_{0.45}$  from the GRB rest frame to the fireball comoving frame. Due to blueshift,  $E_{\text{pk}}$  and the comoving (primed)  $E'_{\text{pk}}$  are related by  $E_{\text{pk}} = E'_{\text{pk}}\delta$ , where  $\delta = 1/[\Gamma(1 - \beta \cos \xi)]$  is the relativistic Doppler factor, and  $\xi$  is the angle between the line of sight and the velocity vector. Similarly, we have  $T_{0.45} = T'_{0.45}/\delta$ . For the isotropic equivalent luminosity we have two possible transformations, according if the fireball is collimated in an angle  $\theta_j > 1/\Gamma$  (“standard” fireball) or if its relevant aperture angle  $\theta_j < 1/\Gamma$  [e.g. it is made by “bullets” (Heinz & Begelman 1999; sub-jets (Toma, Yamazaki & Nakamura, 2005); or cannonballs (e.g. Dar & De Rujula 2004)]. In the former case we have  $L_{\text{iso}} = \delta^2 L'_{\text{iso}}$ , while in the latter  $L_{\text{iso}} = \delta^4 L'_{\text{iso}}$ . This is due to the fact that, for  $\theta_j > 1/\Gamma$ , radiation is collimated in a cone of semiaperture angle  $\theta_j$ , while, if  $\theta_j < 1/\Gamma$ , the collimation angle becomes  $1/\Gamma$ .

For ease of discussion, let us approximate Eq. 9 as  $L_{\text{iso}} \propto E_{\text{pk}}^{3/2} T_{0.45}^{-1/2}$ . It is clear that, for  $\theta_j > 1/\Gamma$ , the same relation holds in the comoving frame: *the  $\delta$  factors cancel out*. Instead, for  $\theta_j < 1/\Gamma$ , we have  $L'_{\text{iso}} \propto \delta^{-2} (E'_{\text{pk}})^{3/2} (T'_{0.45})^{-1/2}$ : there is a rather strong dependence on  $\delta$ .

In other words, Eq. 9 is “Lorentz invariant” only for “normal” fireballs (i.e. those with  $\theta_j > 1/\Gamma$ ). In the opposite case ( $\theta_j < 1/\Gamma$ ) if the  $\Gamma$  factor varies more than a given (small) factor from event to event, then we have a conflict with the tightness of our relation. We can therefore conclude that the standard fireball scenario is favored with respect to models in which we see the entire emitting surface (cannonballs, sub-jets and bullets, of angular extension  $\theta < 1/\Gamma$ ).

If the “Lorentz invariance” can be used as a discriminating guide among the two possible forms of the Ghirlanda relation (favoring its “wind-like” version, which linearly links  $E_\gamma$  and  $E_{\text{pk}}$ ), then we have, from that relation, that the number of relevant photons of the prompt emission (those contributing the most to  $E_\gamma$ ) must be the same in different bursts (see Eq. 6 and Nava et al. 2006). From the  $L_{\text{iso}}-E_{\text{pk}}-T_{0.45}$  relation found in this paper, instead, we derive a relation between the local (and instantaneous) maximum brightness of the fireball, the  $T_{0.45}$  timescale and  $E_{\text{pk}}$ . This relation, in the comoving frame, reads

$$r^2 F' \propto \frac{(E'_{\text{pk}})^{3/2}}{(T'_{0.45})^{1/2}} \rightarrow r^2 \dot{n}'_\gamma \sim r^2 \frac{F'}{E'_{\text{pk}}} \propto \left[ \frac{E'_{\text{pk}}}{T'_{0.45}} \right]^{1/2} \quad (18)$$

where  $r$  is the radius of the fireball when it emits the peak brightness  $F'$  and the photon peak flux  $\dot{n}'_\gamma$ . From this perspective, we can see that the Ghirlanda relation and the relation found here (Eq. 9) are complementary, describing two different aspects (albeit hopefully related) of the GRB physics.

## 8 CONCLUSIONS

GRBs are extremely interesting objects: (i) their nature and physics are still a mystery to solve, and, (ii) GRBs, being the most powerful explosions in the Universe, can serve as a valuable cosmological tool.

An important step forward in the study of GRBs has been recently achieved through the discovery of several correlations among their intrinsic properties.

Through the analysis of a sample of 22 GRBs, we have discovered a new very tight correlation among  $\gamma$ -ray prompt emission properties alone (Sec. 5). The rest frame prompt-emission quantities that we have correlated are: the bolometric corrected energy and luminosity  $E_{\text{iso}}$  and  $L_{\text{iso}}$ , the prompt emission spectrum peak energy  $E_{\text{pk}}$ , the variability of the  $\gamma$ -ray lightcurve  $V$ , and the “high signal” timescale  $T_{0.45}$  (as defined in Sec. 4.1). We have adopted in this paper an improved method to estimate  $V$  and  $T_{0.45}$  from the prompt emission lightcurve. Moreover, we adopted an integral measure of the light curve variability as defined through the ratio  $\Phi = L_{\text{iso}} T_{0.45} / E_{\text{iso}}$ . The number of objects available to find these correlation is unfortunately still small, and a robust physical explanation is still to be found. Bearing that in mind, the main conclusions of our study are:

- Long GRBs with measured redshifts obey a very tight

rest frame multi variable correlation which involves three prompt emission quantities:  $L_{\text{iso}} \propto E_{\text{pk}}^{1.62} T_{0.45}^{-0.49}$  (Eq. [9] and Fig. 3). The scatter of this correlation is comparable to that of the  $E_{\text{iso}}$ ,  $E_{\text{pk}}$  and  $t_{\text{break}}$  (LZ2005; Fig. 1). Nonetheless, the newly found  $L_{\text{iso}}-E_{\text{pk}}-T_{0.45}$  correlation *involves only prompt-emission quantities*.

- The four GRBs (980425, 990712, 010921 and 031203) which populate the low-luminosity tail of the  $L_{\text{iso}}$  distribution of the bursts of our sample, were not included in the derivation of the above correlation. This is because of their arguable nature and/or high uncertainties in their observational parameters. However, with respect to the  $L_{\text{iso}}-E_{\text{pk}}-T_{0.45}$  correlation, they define a low luminosity “branch” (Fig. 6). Whether the origin of this branch is physical or merely a consequence of the lack of spectral data at low energies (as for GRB 031203), is an intriguing question which requires further analysis.

- Other tight correlations among a larger number of prompt emission quantities were also found by our multi variable analysis. For example, we reported a correlation of  $\Phi$  as a function of  $E_{\text{pk}}$ ,  $E_{\text{iso}}$ ,  $T_{0.45}$  and  $V$  ( $\chi_r^2 = 0.62$ ; Eq. 8 and Fig. 2), and of  $E_{\text{iso}}$  as a function of  $E_{\text{pk}}$ ,  $T_{0.45}$  and  $\Phi$  ( $\chi_r^2 = 0.63$ ; Eq. 16). However, these extra variables (with respect to the  $L_{\text{iso}}-E_{\text{pk}}-T_{0.45}$  correlation), only slightly improve the best fit  $\chi_r^2$ , at the cost to include a larger number of variables.

- The tightness of the multi variable correlation  $L_{\text{iso}}-E_{\text{pk}}-T_{0.45}$  allows us to use it as a cosmology-dependent redshift indicator for GRBs. For the concordance cosmological model used here, we presented the formulas necessary to infer pseudo-redshifts given three observables: the bolometric corrected  $P$ ,  $E_{\text{pk}}^{\text{obs}}$ , and  $T_{0.45}^{\text{obs}}$ . This method represents an improvement with respect to previous methods.

- We have re-derived the  $E_{\text{iso}}-E_{\text{pk}}-t_{\text{break}}$  relation (LZ2005) for the 15 GRBs out of our sample with known  $t_{\text{break}}$ . Then, we connected this relation to one equivalent to the  $L_{\text{iso}}-E_{\text{pk}}-T_{0.45}$  relationship ( $E_{\text{iso}}[E_{\text{pk}}, t_{\text{break}}, \Phi]$ ) and found  $t_{\text{break}} \approx 4(\Phi^2/T_{0.45})^{0.6}$  days. This dependence establishes a connection between prompt local quantities ( $\Phi$  and  $T_{0.45}$ , related to the  $\gamma$ -ray lightcurve variability), and a global quantity associated to the afterglow ( $t_{\text{break}}$ ), suggesting that  $t_{\text{break}}$  (and  $\theta_j$ ) could be determined mainly by the prompt emission local properties.

- In the context of the standard fireball scenario, the  $L_{\text{iso}}-E_{\text{pk}}-T_{0.45}$  correlation is roughly “Lorentz invariant”. This allows us to go deeper and relate it to the local comoving fireball surface brightness associated to the fireball area that the observer sees. Therefore, while the Ghirlanda relations seems to be related to a global feature of the fireball (the number of emitted photons), the  $L_{\text{iso}}-E_{\text{pk}}-T_{0.45}$  relationship could be describing a local feature of the fireball related to its brightness.

The results found in this paper reveal the existence of tight correlations among quantities related to the prompt emission of long GRBs. On one hand, these correlations will contribute to understand better the physics of GRBs. On the other hand, they can be used to infer pseudo-redshifts with good accuracy for hundreds of GRBs or, for those events with known  $z$ , serve as “standard candles” for cosmographic purposes. The main challenge is the acquirement of observational data related to the  $\gamma$ -ray prompt light curves and

spectral distributions. In particular, detector flux sensitivities extending to energies as high as 500–1000 keV are crucial, also for revealing the effects of possible observational bias.

## ACKNOWLEDGMENTS

We thank the anonymous referee for insightful comments and Davide Lazzati for discussions. We also thank Giuseppe Malaspina for technical support and Yair Krongold for useful advice on X-ray spectrum analysis. V.A.-R. gratefully acknowledges the hospitality extended by Osservatorio Astronomico di Brera. We thank the Italian INAF and MIUR for funding (Cofin grant 2003020775\_002).

## REFERENCES

- Amati L., Frontera F., Vietri M., et al., 2000, *Science*, 290, 953
- Amati L. et al., 2002, *A&A*, 390, 81
- Amati L., 2004, *astro-ph/0405318*
- Andersen M.I., et al., 2000, *A&A*, 364, L54
- Andersen M.I., Masi G., Jensen B.L., & Hjorth J., 2003, *GCN Circ.*, 1993
- Atteia J.-L., 2003, *A&A*, 407, L1
- Atteia, J.-L., Kawai. N., Vanderspek, R., et al. 2005, *ApJ*, 626, 292
- Band D., Matteson J., Ford L. et al., 1993, *ApJ*, 413, 281
- Barraud, C., Olive, J.-F., Lestrade, J.P., et al. 2003, *A&A*, 400, 1021
- Barth A.J., Sari R., Cohen M.H., et al., 2003, *ApJ*, 584, L47
- Berger E., Kulkarni S.R., Bloom J.S., et al., 2002, *ApJ*, 581, 981
- Berger E., Kulkarni S.R., Pooley G., et al., 2003, *Nature*, 426, 154
- Bersier D., et al., 2003, *GCN*, 2544
- Blain A. W. & Natarajan P., 2000, *MNRAS*, 312, L35
- Bloom J.S., Frail D. A. & Sari R., 2001, *AJ*, 121, 2879
- Bloom J.S., Frail D. A. & Kulkarni S. R., 2003, *ApJ*, 594, 674
- Blustin A.J. et al., 2005, *ApJ*, 637, 901
- Bromm V. & Loeb A., 2002, *ApJ*, 575, 111
- Bjornsson G., Hjorth J., Jakobsson P., Christensen L., & Holland S., 2001, *ApJ*, 552, L121
- Costa E. et al., 1997, *Nature*, 387, 783
- Dai Z.G., Liang E.W. & Xu D., 2004, *ApJ*, 612, L101
- Dar, A. & de Rujula, A., 2004, *Phys. Rep.*, 405, Issue 4, p. 203
- Djorgovsky S.G., Kulkarni S.R., Bloom J.S., Frail D.A., et al., 1997, *GCN*, 289
- Djorgovsky S.G., Kulkarni S.R., Bloom J.S., Goodrich R., Frail D.A., Piro L., & Palazzi E., 1998, *ApJ*, 508, L17
- Djorgovsky S.G., Frail D.A., Kulkarni S.R., Bloom J.S., Odewahn S.C., & Diercks A., 2001, *ApJ*, 562, 654
- Djorgovsky S.G., et al., 2001, *GCN Circ.*, 1108
- Fenimore E. E. & Ramirez-Ruiz E., 2000, preprint (*astro-ph/0004176*)
- Firmani C., Avila-Reese V., Ghisellini G. & Tutukov A. V., 2004, *ApJ*, 611, 1033
- Firmani C., Ghisellini G., Ghirlanda G. & Avila-Reese V., 2005, *MNRAS*, 360, L1
- Foley R.J., Chen H.-W., Bloom J., & Prochaska J.X., 2005, *GCN Circ*, 3483
- Frail D. A. et al., 1997, *Nature*, 389, 261
- Frail D. A. et al., 2001, *ApJ*, 562, L55
- Friedman A. S. & Bloom J. S., 2005, *ApJ*, 627, 1
- Frontera F. et al., 2001, *ApJ*, 550, L47
- Galama T. J., 1999, *GCN Circ.*, 388
- Ghisellini G., Ghirlanda G., Firmani C., Lazzati D. & Avila-Reese V., 2005, *Il Nuovo Cimento*, in press
- Ghirlanda G., Ghisellini G. & Lazzati D. 2004a, *ApJ*, 616, 331 (*GGL2004*)
- Ghirlanda G., Ghisellini G., Lazzati D. & Firmani, C., 2004b, *ApJ*, 613, L13
- Ghirlanda G., Ghisellini G., Firmani C., Celotti A., & Bosnjak Z., 2005, *MNRAS*, 360, L45
- Ghirlanda G. et al., 2005a, *A&A* submitted (*astro-ph/0511559*)
- Golenetskii S., et al., 2004, *GCN Circ.*, 2754
- Greiner J., Guenther E., Klose S., & Schwarz R., 2003a, *GCN Circ.*, 1886
- Greiner J., Peimbert M., Esteban C. et al., 2003a, *GCN Circ.*, 2020
- Guidorzi C. et al., 2005, *MNRAS*, 363, 315
- Heinz, S. & Begelman, M.C., 1999 *ApJ*, 527, L35
- Hjorth J., Andersen M.I., Cairo L.M. et al., 1999, *GCN Circ.*, 219
- Hjorth J., Moller P., Gorosabel J. et al. 2003, *ApJ*, 597, 699
- Klose S., Greiner J., Rau A. et al., 2004, *AJ*, 128, 1942
- Israel G., Marconi G., Covino S. et al., 1999, *A&A*, 384, L5
- Jakobsson P., Hjorth J., Fynbo J.P.U. et al., 2003, *A&A*, 408, 941
- Jakobsson P., Hjorth J., Fynbo, J.P.U., et al., 2004, *A&A*, 427, 785
- Jimenez R., Band D. & Piran T., 2001, *ApJ*, 561, 171
- Kulkarni S. R., et al., 1998, 393, 35
- Kulkarni S. R., Djorgovsky, S. G., Odewahn S. C. et al., 1999, *Nature*, 398, 389
- Lamb D.Q. & Reichart D.E., 2000, *ApJ*, 536, 1
- Lamb D. Q. et al., 2005, White Paper submitted to the Dark Energy Task Force, *astro-ph/0507362*
- Liang E. & Zhang B., 2005, *ApJ*, 633, 611, (*LZ2005*)
- Lloyd-Ronning N.M., Fryer C.L. & Ramirez-Ruiz E., 2002, *ApJ*, 574, 554
- Lloyd-Ronning N. & Ramirez-Ruiz E., 2002a, *ApJ*, 576, 101
- Mereghetti S. & Gotz D., 2003, *GCN Circ.*, 2460
- Nava L., Ghisellini G., Ghirlanda G., Tavecchio F., & Firmani C., 2006, *A&A*, in press (*astro-ph/0511499*)
- Norris J. P., Marani G. F. & Bonnell J. T., 2000, *ApJ*, 534, 248
- Paciesas et al. 1999, *ApJS*, 122, 465
- Paczynski B., 1998, *ApJ*, 494, L45
- Piro L. et al., 2005, *ApJ*, 623, 314
- Press W.H. et al., 1999, *Numerical Recipes in C*, Cambridge University Press, 661
- Price P., et al., 2002, *ApJ*, 573, 85
- Reichart D., Lamb, D. Q., Fenimore, E. E., Ramirez-Ruiz, E., Cline, & Th. L., Hurley, K., 2000, *ApJ*, 552, 57

- Rhoads J.E., 1997, ApJL, 487, L1  
Rol E., Vreeswijk P., & Jaunsen A., 2003, GCN Circ., 1981  
Salmonson J.D. & Galama T. J., 2002, ApJ, 569, 682  
Sakamoto, T., Lamb, D.Q., Kawai, N., et al. 2005, ApJ, 629, 311  
Sari R., Piran T. & Halpern J.P., 1999, ApJ, 519, L17  
Sazonov, S. Yu.; Lutovinov, A. A.; Sunyaev, R. A., 2004, Nature, 430, 646  
Schaefer B.E., 2003, ApJ, 583, L67  
Schaefer B. E., Deng M., & Band D. L., 2001, ApJ, 563, L123  
Stanek K.Z., Garnavich P.M., Nutzman P.A., et al., 2005, ApJ, 626, L5  
Tinney C., et al., 1998, IAU Circ., 6896  
Toma, K., Yamazaki, R., & Nakamura, T., 2005, ApJ, 635, 481 ApJS, 148, 175  
Totani T., 1997, ApJ, 486, L71  
van Paradijs J. et al., 1997, Nature, 386, 686  
Vreeswijk P.M., Rol E., Hjorth J., et al., 1999, GCN Circ., 496  
Vreeswijk P.M., Fruchter A., Kaper L., et al., 2001, ApJ, 546, 672  
Vreeswijk P.M., et al., 2003, GCN, 1785  
Watson D., Vaughan S. A., Willingale R. et al., 2006, ApJ, 636, 381  
Weidinger M., Fynbo J.P.U., Hjorth J., Gorosabel J., Klose S., 2003, GCN 2196  
Wiersema K. et al., 2004, GCN, 2800  
Wijers R. A. M. J., Bloom J.S., Bagla J. S. & Natarajan P., 1998, MNRAS, 249, L13  
Xu D., 2005, preprint (astro-ph/0504052)  
Xu D., Dai Z. G. & Liang E. W., 2005, ApJ, 633, 603  
Yamazaki R, Yonetoku D., Nakamura T., 2003, ApJ, 594, L79  
Yonetoku D. et al., 2004, ApJ, 609, 935